Article

Not peer-reviewed version

Post-Embryonic Gonad Development in the Capital-Breeding Seed Beetle *Zabrotes subfasciatus* (Bruchinae): A Morphological View

Juliana Ramos Martins , Márcia Maria Gentile Bitondi , Sílvia de Oliveira Miranda , Talita Sarah Mazzoni , Angel Roberto Barchuk *

Posted Date: 30 July 2026

doi: 10.20944/preprints202607.2205.v1

Keywords: ovary; ovariole; testis; seed beetle; development

 doi:10.20944/preprints202607.2205.v1

Article

Post-Embryonic Gonad Development in the Capital-Breeding Seed Beetle *Zabrotes subfasciatus* (Bruchinae): A Morphological View

Juliana Ramos Martins [1], Márcia Maria Gentile Bitondi [2], Sílvia de Oliveira Miranda [1], Talita Sarah Mazzoni [1] and Angel Roberto Barchuk [1,*]

[1] Departamento de Biologia Celular e do Desenvolvimento, Instituto de Ciências Biomédicas, Universidade Federal de Alfenas, UNIFAL-MG, Alfenas, Minas Gerais, Brazil

[2] Departamento de Biologia, Faculdade de Filosofia, Ciências e Letras de Ribeirão Preto, Universidade de São Paulo, USP, Ribeirão Preto, São Paulo, Brazil

* Correspondence: barchuk@unifal-mg.edu.br or arbarchuk@yahoo.com

Simple Summary

Seed beetles are important pests of stored legumes, but little is known about how their reproductive organs develop before adulthood. This study examined the formation of ovaries and testes in *Zabrotes subfasciatus*, a bean weevil whose adults depend mainly on reserves accumulated while feeding inside seeds as larvae. Using stereomicroscopy, histology, and scanning electron microscopy, we found that gonad development starts during larval life but that the main changes leading to reproductive readiness occur during late metamorphosis, especially between the pupal and pharate-adult stages. In females, this period includes the organization of the ovaries, the appearance of developing oocytes, follicular cells, trophic cords, and the first signs of yolk deposition, showing that egg maturation begins before adult emergence. In males, the testes also mature early, with advanced sperm development already evident before emergence. These results help explain why newly emerged adults of this pest can become reproductively active quickly and provide useful information for future studies on reproductive biology and pest-management strategies.

Abstract

Post-embryonic gonad development is essential for determining when insects acquire reproductive competence, yet it remains poorly characterized in Bruchinae seed beetles. This study examined ovarian and testicular development in the capital-breeding bean weevil *Zabrotes subfasciatus* from larval stages to four-day-old adults using stereomicroscopy, light microscopy, and scanning electron microscopy. Female gonads were already recognizable in larvae as ovaries with three ovarioles dominated by a proliferative germarial region and posterior duct-like domains. During pharate-pupal and pupal development, these structures remained largely previtellogenic but showed ductal integration associated with future calyx formation. The main ovarian reorganization occurred in pharate adults, when terminal filaments, individualized oocytes, follicular cells, trophic cords, and a germarium-vitellarium transition became evident; eosinophilic inclusions consistent with initial yolk suggest that vitellogenesis begins before emergence. Male gonads also differentiated early, with larval testes containing germ stem cells, spermatogonia, spermatocytes, spermatids, cyst cells, and the internal portion of efferent ducts. From the pharate-pupal stage onward, spermiogenesis intensified, and four-day-old adults displayed a fully organized reproductive tract. These findings show that gonad development begins during larval life but attains functional organization mainly during late metamorphosis, supporting rapid reproductive readiness in this capital-breeding pest.

Keywords: ovary; ovariole; testis; seed beetle; development

 doi:10.20944/preprints202607.2205.v1

1. Introduction

Seed beetles of the subfamily Bruchinae (Coleoptera: Chrysomelidae) are phytophagous insects strongly associated with leguminous plants (Fabaceae). Their larvae develop endophagously inside seeds, where they complete most of their growth while consuming cotyledonary and embryonic tissues. This seed-confined development underlies the economic importance of many Bruchinae as pests of field-grown and stored legumes and also makes the group a useful model for studying how specialized life histories shape developmental and reproductive strategies (Southgate, 1979; Cruz et al., 2026).

Despite extensive information on host use, oviposition behaviour, taxonomy, and life-history variation in Bruchinae (Southgate, 1979; Kingsolver, 2004), the post-embryonic development of their reproductive organs remains poorly characterized. Developmental timing has been described for some seed beetles, including *Callosobruchus maculatus* and *Acanthoscelides macrophthalmus*, but detailed comparative accounts of ovarian and testicular differentiation are still scarce (Kutcherov, 2020; Wu et al., 2012). This gap is important because gonad development determines when newly emerged adults become reproductively competent, a particularly relevant issue for seed beetles whose adult stage may be short and only weakly dependent on feeding. The relationship between nutrition and reproduction provides a central framework for interpreting this developmental timing. In income-breeding insects, reproductive maturation is closely linked to nutrients acquired during adult life, as demonstrated in the beetles *Tenebrio molitor* (Gerber, 1967) and *Nicrophorus* spp. (Wilson and Knollenberg, 1984). In contrast, capital breeders rely mainly on reserves accumulated before reproduction, so gonadal maturation is expected to begin earlier and to progress during late juvenile or metamorphic stages (Jönsson, 1997). Many Bruchinae fit this latter strategy because adults often feed little or not at all, and their reproductive output depends largely on larval resources. Accordingly, gonadal maturation in these beetles may be advanced, compressed, or coordinated with metamorphosis rather than delayed until after emergence (Southgate, 1979; Miranda et al., 2025).

Zabrotes subfasciatus (Boheman, 1833) is a bruchine seed beetle native to Central and South America and now widely distributed in tropical bean-growing regions (Lucas, 1858; Valencia et al., 1986; Schoch et al., 2020). Females lay eggs on the seed surface, larvae bore into the seed after hatching, and development proceeds internally until pupation and adult emergence. Under favourable laboratory conditions, adults usually emerge about 26 days after oviposition at 30–35 °C (Corrêa et al., 2021). Adult feeding and water intake appear to be facultative, reinforcing the view that this species depends primarily on reserves accumulated during larval development to support reproduction (Howe and Currie, 1964; Southgate, 1979; Kingsolver, 2004; Corrêa et al., 2020).

Previous work on *Z. subfasciatus* has shown that ovarian activation depends on both host seeds and male presence and that vitellogenesis begins before or soon after adult emergence (Miranda et al., 2025). However, the sequence by which larval gonadal primordia are transformed into functional adult ovaries and testes remains unknown. Addressing this question is relevant for three reasons. First, it clarifies how reproductive organ ontogeny proceeds in an insect whose immature development is spatially and nutritionally constrained inside a seed. Second, because many Bruchinae are economically important pests, understanding the timing of gonadal maturation may help explain their rapid reproductive potential and inform future pest-management approaches (Tuda, 2011). Third, it remains uncertain whether seed beetles follow the generalized gonadal developmental patterns described for other holometabolous beetles or whether their capital-breeding ecology is associated with modifications in the timing and organization of gonad development.

Based on the reproductive biology of *Z. subfasciatus* and on previous evidence that adult females possess three telotrophic meroistic ovarioles with early vitellogenic activity (Miranda et al., 2025), we hypothesised that gonadal primordia are established during larval life and that maturation progresses through metamorphosis, allowing both ovaries and testes to approach functional readiness by adult emergence. Accordingly, this study aimed to describe the morphological and histological progression of gonad development in *Z. subfasciatus* from larval to adult stages, with

 doi:10.20944/preprints202607.2205.v1

emphasis on germ-cell proliferation, somatic differentiation, and the onset of gametogenic organization in both sexes.

2. Materials and Methods

2.1. Beetle Husbandry and Sampling

The *Z. subfasciatus* individuals used in this study originated from a stock population of approximately 6,000 individuals, initially collected from bean seeds in Ribeirão Preto, São Paulo, Brazil, and maintained on bean (*P. vulgaris*, "carioquinha" variety) seeds in the laboratory since 1997. According to Souza et al. (2008), Brazilian populations of *Z. subfasciatus* exhibit low genetic differentiation and weak geographic structure. To minimize potential inbreeding effects, individuals collected from bean seeds in Poços de Caldas and Alfenas, Minas Gerais, Brazil, have been incorporated into the stock population approximately every three months since 2007. The colony was maintained on bean seeds at 22 ± 5 °C and 70 ± 15% relative humidity, under dark conditions (Corrêa et al., 2020, 2021). Additional information on the biology of this species is available in Bondar (1937), Teixeira et al. (2009), Teixeira and Gris (2011), Teixeira and Zucoloto (2012), and Cruz et al. (2026).

Larvae (14 days after egg laying), pharate pupae (20-22 days), pupae displaying white bodies (20-22 days), and pharate adults exhibiting dark pigmentation (24-25 days) were carefully extracted from the seeds using a scalpel for cutting and No. 5 watchmaker's forceps for insect removal. Adults were obtained from a population maintained in beans. For dissection, individuals were placed in a watch glass containing phosphate-buffered saline (PBS). Using No. 5 watchmaker's forceps, No. 2 entomological pins, and a Stemi 305 stereomicroscope (Zeiss), the abdominal cuticle was opened and internal tissues were removed. The ovaries and testes of developing and adult beetles were isolated from surrounding tissues and subsequently fixed.

2.2. Histology

Whole individuals were processed following the protocol from Lussier et al. (2023) with some adjustments. Individuals were fixed in Schaffer fixative (1 part 37% formaldehyde to 2 parts 90% ethanol) mixed with depilatory cream containing calcium thioglycolate (DepiRoll Resistance®) in a 2:1 ratio, and maintained for 5 days at 4 °C. The samples were then washed in PBS, small holes were made in the cuticle using an entomological pin, and they were incubated in a modified Alcohol-Formalin-Acetic acid Fixative (Kiernan, 2015) (12 parts 80% ethanol, 4 parts 37% formaldehyde, and 1 part glacial acetic acid) for two days at 4°C. Dissected ovaries and testes were fixed according to Karnovsky (1965) for 24 hours. After fixation, samples were dehydrated in ethanol (70%, 80%, 90%, and 95%, each for two 30-minute intervals), and embedded in glycol methacrylate (Leica Historesin) using a stepwise infiltration process, as follows: 2 parts 95% ethanol and 1 part Historesin infiltration solution for 1 hour; 1 part 95% ethanol and 1 part Historesin infiltration solution for 1 hour; 1 part 95% ethanol and 2 parts Historesin infiltration solution for 1 hour; only Historesin infiltration solution for 2 days at 4°C and 3 days at room temperature. The samples were sectioned to a thickness of 5 µm with a Leica Rotary Microtome and all sections were stained with Harris hematoxylin and eosin (Harris, 1900) (H&E). Micrographs of the sections were taken using a Nikon Eclipse 80i microscope equipped with a digital camera and Nis-Element 3.1 imaging software.

2.3. Scanning Electron Microscopy (SEM)

Dissected adult ovaries and testes were fixed in Karnovsky's solution (1965) for 24 h.

Samples were then washed twice with 1x PBS and post-fixed in 1% osmium tetroxide for 1 hour. For removal of osmium remnants, samples were again washed twice with PBS and once with deionized water, each for a period of 10 min. Then a serial dehydration was done with increasing concentrations of ethanol (10, 30, 50, 70, 90, 100%). Each ethanol bath was done twice, for 10 minutes. Thereafter, samples were dried using a CO2 critical point drier (Tousimis Autosamdri®-815). Specimens were finally coated with a gold sputter coater (Denton Vacuum) for a coat of 20 nm.

 doi:10.20944/preprints202607.2205.v1

Coated samples were observed and photographed using a scanning electron microscope (TESCAN-MIRA4 FEG) using an Everhart-Thornley Secondary Electrons Detector and an In-Beam Secondary Electrons Detector at 10kV. Images were captured at the Centro de Microscopia, Universidade Federal de Alfenas, Minas Gerais, Brazil.

3. Results

3.1. General External Morphology of the Developing Gonads of Zabrotes Subfasciatus

We obtained stereomicroscope, light-microscope, and scanning electron-microscope images to document the general morphology of gonad development throughout the post-embryonic ontogeny of *Z. subfasciatus*, from larval to adult stages. Under the stereomicroscope, the ovary of a 14-day-old larva appears as a small, three-lobed, opaque structure formed by the ovarioles and attached posteriorly. In each ovariole, the anterior region is slightly broader than the posterior portion, a pattern that becomes more evident in the subsequent pharate-pupal stage (Figure 1, middle column). From the pupal stage onward, the ovaries become more elongated and mostly translucent, although distinct functional domains are still not clearly visible in pupae. Such compartmentalization becomes evident only in pharate adults, in which the ovarioles can already be distinguished into proliferative and early vitellogenic regions, even though the anterior portion remains relatively translucent. In adults, this organization is fully evident, with a clear separation between the proliferative region and the different stages of vitellogenesis.

Under the stereomicroscope, the testes of a 14-day larva appear larger than the ovaries, forming two paired opaque spheres (testicular follicles) connected by thin strands of tissue (Figure 1, right column). This general appearance is maintained through the pupal stage. In pharate adults, however, the testes are already connected to a well-developed posterior tract, similar to that observed in adults.

3.2. Histological Organization of the Larval Ovary of Zabrotes subfasciatus

Light microscopy revealed that the ovaries of *Z. subfasciatus* larvae (14 days after oviposition) are in the posterior-dorsal region of the abdomen and are surrounded by fat body tissue (Figure 2A-C). The intimate association between the gonad and fat body is typical of holometabolous insects and reflects the metabolic support required for germ-cell proliferation and differentiation. The ovarioles are differentiated into two main regions: a larger anterior region, the germarium, and a posterior duct-like region (Figure 2D, G). These regions display distinct histomorphologies consistent with a germarium anteriorly and a posterior epithelial domain, based on H&E criteria (region identities remain provisional pending molecular validation). The germarium is densely populated with germ cells interspersed with somatic interstitial cells and is enclosed by an inner peritoneal sheath (Figure 2D-G). Anteriorly, the germarium continues into a transition zone to the terminal filament (Figure 2E), whereas posteriorly it extends into the duct-like region, which is composed of epithelial-like cells (Figure 2D, G). Posteriorly, the duct-like regions of the three ovarioles converge and appear to contribute to the final organization of the calyx (see Figures 4B and 5C).

 doi:10.20944/preprints202607.2205.v1

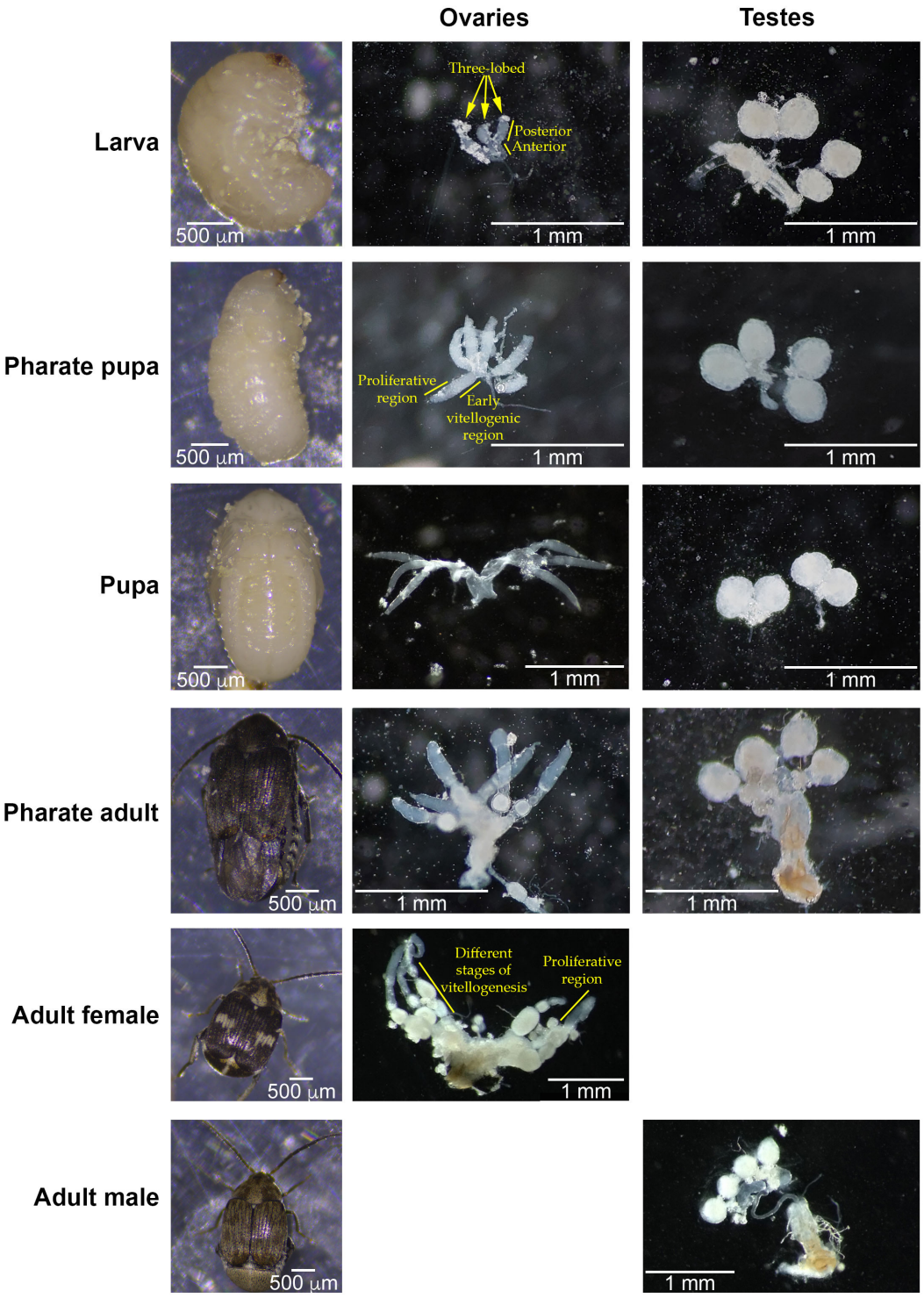

Figure 1. External morphology of the ovary and testis across post-embryonic developmental stages of *Zabrotes subfasciatus*. Larva, 14 days after egg laying; pharate pupa, 20–22 days; pupa, 20–22 days; pharate adult, 24–25 days. Whole individuals and dissected gonads were photographed using a ZEISS Stemi 305 stereomicroscope equipped with an Axiocam 105 colour camera and ZEN 3.7 software. The larval image shows a single ovary, whereas the remaining stages show both ovaries.

 doi:10.20944/preprints202607.2205.v1

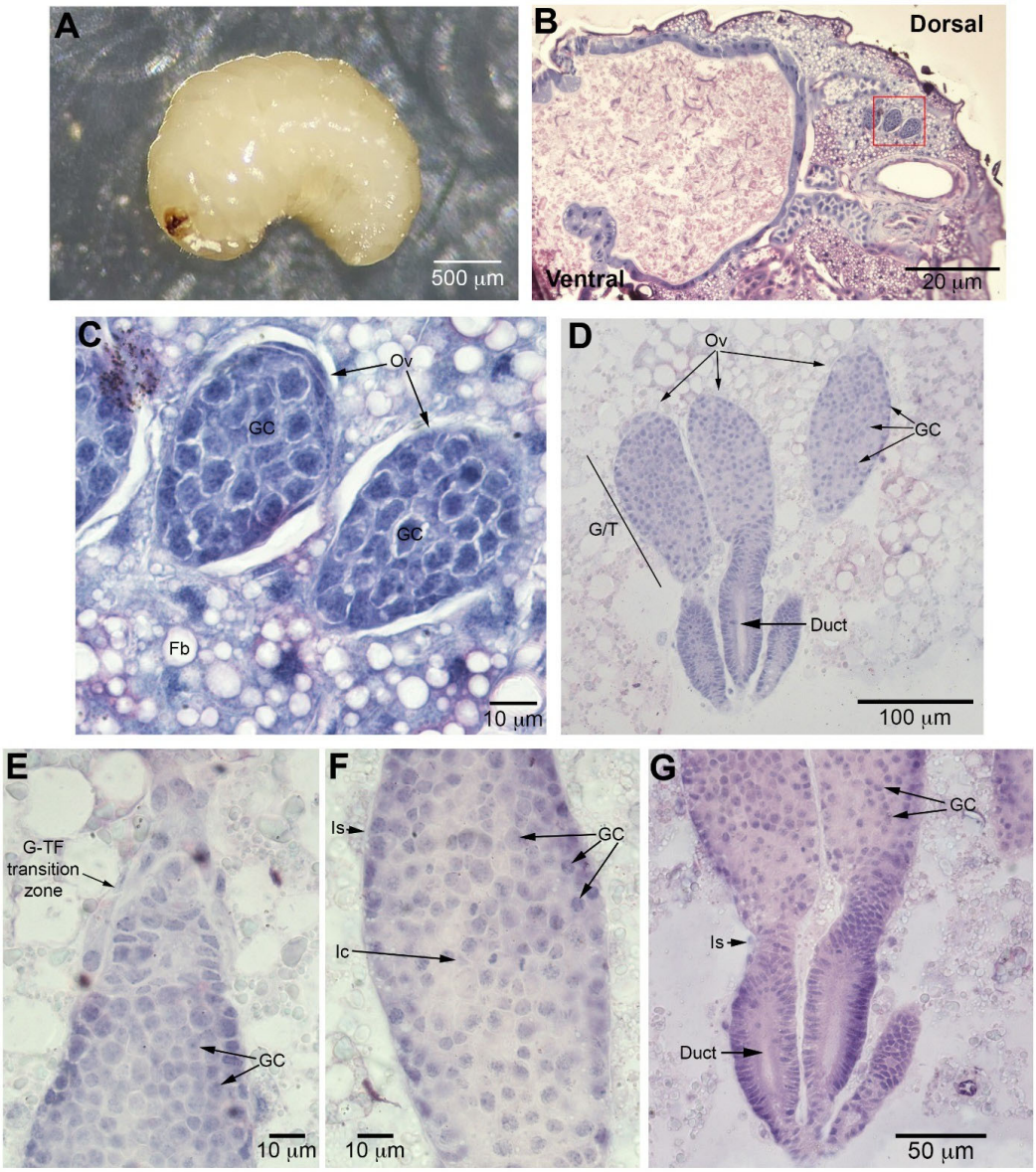

Figure 2. Histological organization of the larval (14 days after egg laying) ovary of *Zabrotes subfasciatus*. A) Larva photographed using a ZEISS Stemi 305 stereomicroscope equipped with an Axiocam 105 colour camera and ZEN 3.7 software. Larval bodies (B and C, longitudinal and transverse sections, respectively) and dissected ovaries (D–G) were embedded in Historesin, sectioned at 5 µm, stained with haematoxylin and eosin, and imaged using a Nikon Eclipse 80i microscope equipped with a digital camera and NIS-Elements 3.1 software. B) Longitudinal section of a larval body highlighting the anatomical location of the ovary (red label). C–G, magnified views of distinct sections from the red-labelled area indicated in B. Ov, ovariole; GC, germ cells; Fb, fat body cells; G/T, germarium/tropharium; G/TF, germarium/terminal filament; Is, inner sheath; Ic, interstitial cell.

The organization of the pharate-pupal ovary (pre-pupa; 20-22 days after egg laying) remains broadly similar to that observed in 14-day-old larvae (Figure 3), although the germarium is noticeably enlarged at this stage (compare Figures 2D and 3D) and contains syncytial cells (Figures 3D, E). In addition, the posterior duct-like regions of the three ovarioles, which contain mitotically active cells (Figure 3E), converge and extend into a single duct-like structure that is consistent with a calyx primordium; continuity to the adult calyx was not directly demonstrated. (Figure 3D). Thus, although

 doi:10.20944/preprints202607.2205.v1

the ovary still lacks the distinct compartmentalization observed in pharate adults, the pharate-pupal stage already exhibits structural rearrangements indicative of the early stages of ovariole maturation.

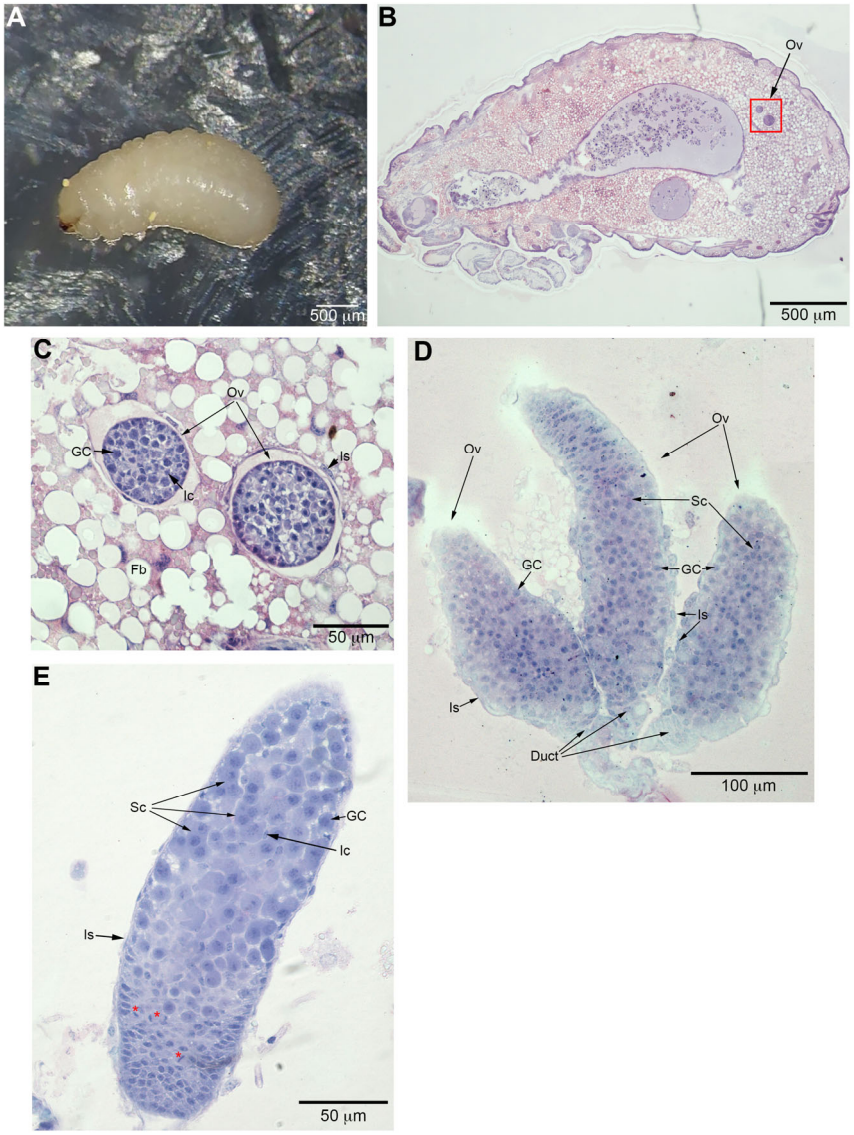

Figure 3. Histological organization of the pharate-pupal (pre-pupa; 20–22 days after egg laying) ovary of *Zabrotes subfasciatus*. A) Pharate pupa photographed using a ZEISS Stemi 305 stereomicroscope equipped with an Axiocam 105 colour camera and ZEN 3.7 software. Pharate-pupal bodies (B and C, longitudinal and transverse sections, respectively) and dissected ovary (D) and ovariole (E) were embedded in Historesin, sectioned at 5 µm, stained with haematoxylin and eosin, and imaged using a Nikon Eclipse 80i microscope equipped with a digital camera and NIS-Elements 3.1 software. B) Longitudinal section of a pharate-pupal body highlighting the anatomical location of the ovary (red label). Ov, ovarioles; GC, germ cells; Fb, fat body cells; Is, inner sheath; Ic, interstitial cell; Sc, syncytial cells; *, dividing cells.

3.3. Histological Organization of the Pupal and Pharate-Adult Ovary of Zabrotes subfasciatus

In early pupae (20-22 days after egg laying), the ovarioles of female *Z. subfasciatus* remain relatively undifferentiated when compared with those of pharate adults, although important structural changes are already evident (Figure 4). At this stage, the ovariole is elongated and dominated by a conspicuous germarium containing densely packed germ cells and syncytial elements, indicating ongoing cellular proliferation and early differentiation. However, not clearly

 doi:10.20944/preprints202607.2205.v1

delimited vitellogenic regions are yet apparent, suggesting that the ovary is still in a previtellogenic state. By the pharate-adult stage (24-25 days after egg laying), the ovarioles display a marked increase in structural organization (Figure 5). The anterior terminal filament becomes readily distinguishable (Figure 5B), and the germarium is more clearly defined. Posterior to this region, developing oocytes can be recognized and are associated with follicular cells and trophic cords (Figure 5D), revealing the onset of the telotrophic organization characteristic of the adult ovary. The duct-like structure observed in prior phases are now only a small pedicel connecting the vitellarium to the newly formed calyx (Figure 5C). The developing vitellarium contains some oocytes showing a conspicuous germinal vesicle, karyosome, and initial yolk deposition, indicating that vitellogenesis begins before adult emergence (Figure 5D-F). These observations show that the transition from the pupal to the pharate-adult stage encompasses the key morphological events that establish the functional compartmentalization of the ovarioles in this species.

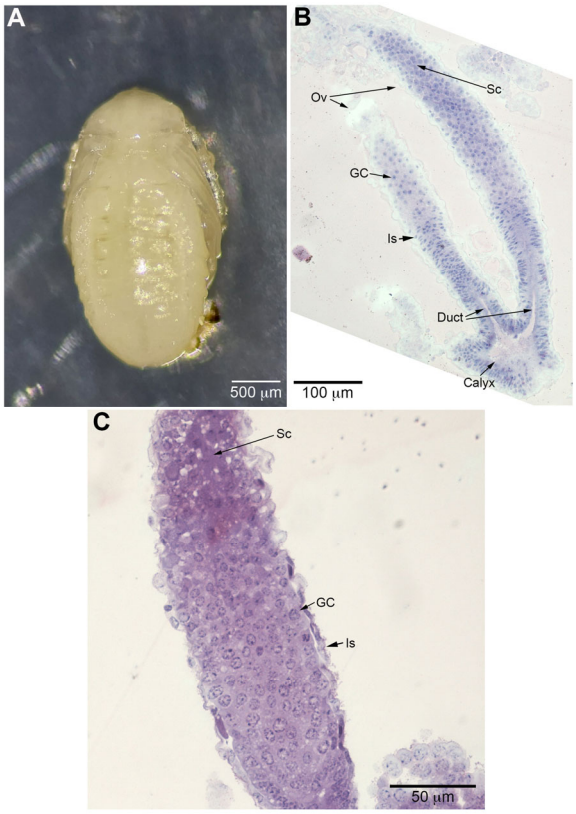

Figure 4. Histological organization of the pupal (20–22 days after egg laying) ovary of *Zabrotes subfasciatus*. A) Pupa photographed using a ZEISS Stemi 305 stereomicroscope equipped with an Axiocam 105 colour camera and ZEN 3.7 software. Dissected ovary (B) and ovariole (C) were embedded in Historesin, sectioned at 5 µm, stained with haematoxylin and eosin, and imaged using a Nikon Eclipse 80i microscope equipped with a digital camera and NIS-Elements 3.1 software. Sc, syncytial cells; GC, germ cells; Is, inner sheath.

 doi:10.20944/preprints202607.2205.v1

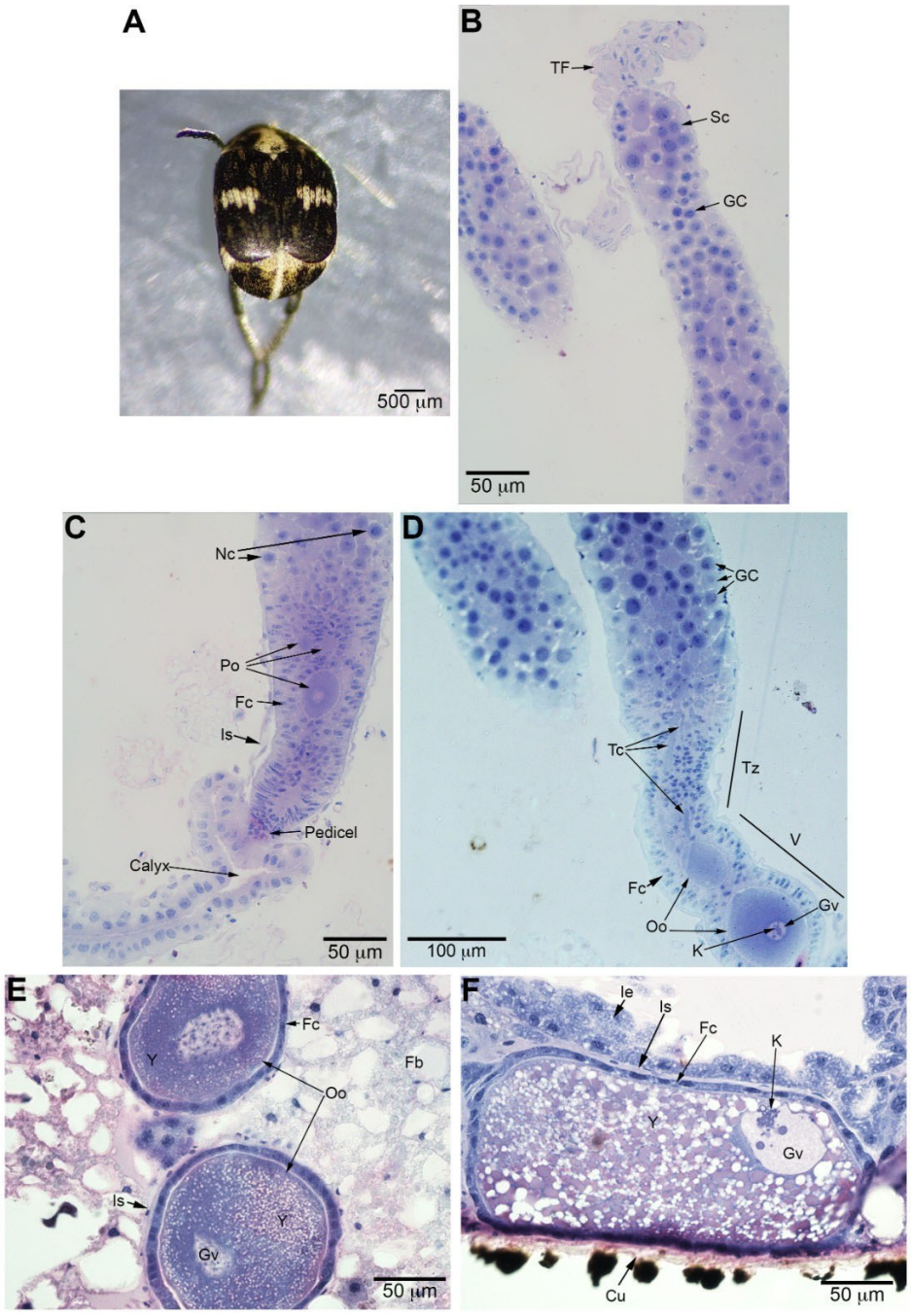

Figure 5. Histological organization of the pharate-adult (24–25 days after egg laying) ovary of *Zabrotes subfasciatus*. A) Pharate adult photographed using a ZEISS Stemi 305 stereomicroscope equipped with an Axiocam 105 colour camera and ZEN 3.7 software. Dissected ovaries (B–D) and whole bodies (E and F, transverse and longitudinal sections, respectively) were embedded in Historesin, sectioned at 5 µm, stained with haematoxylin and eosin, and imaged using a Nikon Eclipse 80i microscope equipped with a digital camera and NIS-Elements 3.1 software. TF, terminal filament; Sc, syncytial cells; GC, germ cells; Nc, nurse cell; Po, Pro-oocytes; Oo, oocytes; Fc, follicular cell; Tc, trophic cord; Tz, transition zone; V, vitellarium; Gv, germinal vesicle; K, karyosome; Y, yolk; Is, inner sheath; Ie, intestinal epithelium; Fb, fat body; Cu, cuticle.

 doi:10.20944/preprints202607.2205.v1

3.4. Organization of the Adult Ovary of Zabrotes subfasciatus

Light microscopy revealed that the ovary of a four-day-old *Z. subfasciatus* female maintained on beans in the presence of males, under optimal conditions for egg production (Miranda et al., 2025), displays morphologically distinct ovariole regions -the terminal filament, germarium/tropharium, transition zone, and vitellarium- based on H&E and SEM criteria. Oocytes within the vitellarium are present at different developmental stages, from pro-oocytes (primary oocytes) to oocytes at advanced stage of differentiation, exhibiting progressive yolk accumulation (Figure 6).

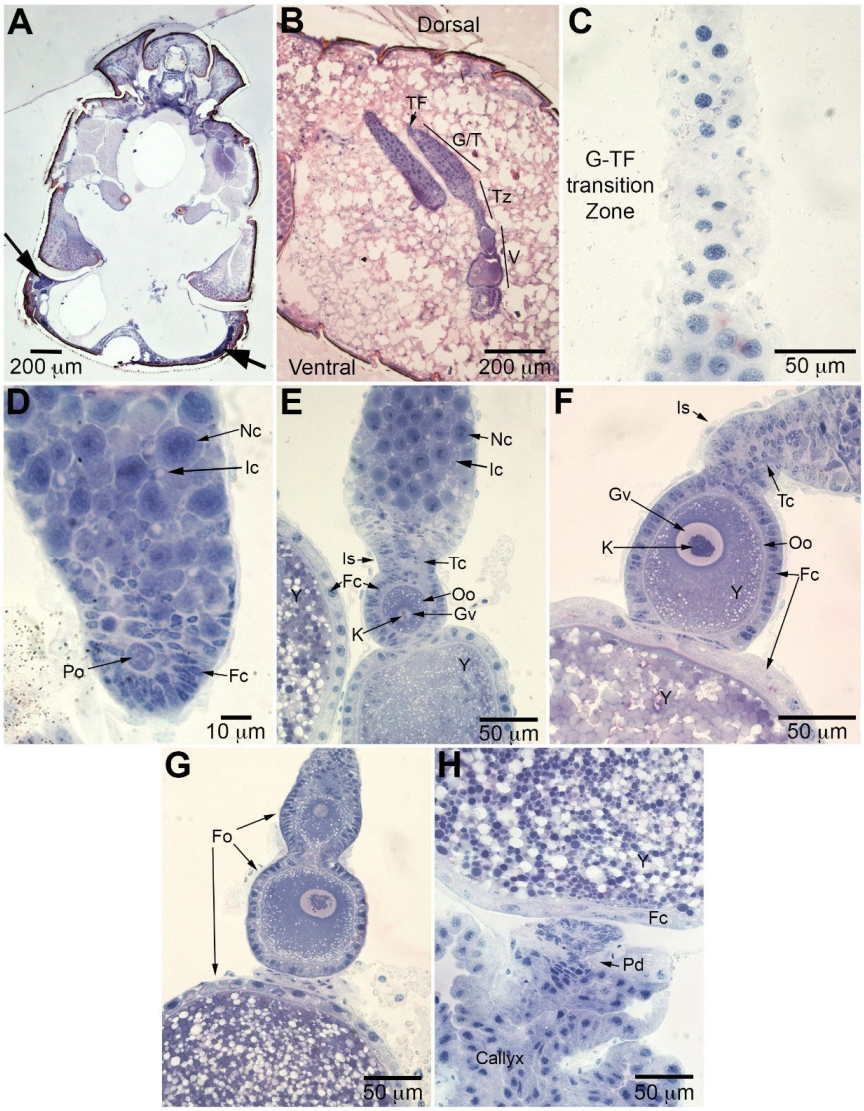

Figure 6. Structural organization of the ovary in a four-day-old *Zabrotes subfasciatus* adult. Whole bodies (A and B, frontal and longitudinal sections, respectively) and dissected ovaries (C-H) were embedded in Historesin, sectioned at a thickness of 5 µm, stained with hematoxylin and eosin, and imaged using a Nikon Eclipse 80i microscope equipped with a digital camera and NIS-Elements 3.1 software. Arrows in A point to ovary pair localization. TF, terminal filament; G-TF, germarium-terminal filament; V, vitellarium; Nc, nurse cell; Ic, interstitial cell; Po, Pro-oocyte; Fc, follicular cell; Is, inner sheath; Tc, trophic cord; Oo, oocyte; Gv, germinal vesicle; K, karyosome; Y, yolk; Fo, follicles; Pd, Pedicel.

 doi:10.20944/preprints202607.2205.v1

Scanning electron-microscope observations further distinguished the major ovariole regions, including the germarium/tropharium, the vitellarium with developing oocytes, and the adult calyx. Detailed images of the external morphology of the terminal filaments were also obtained (Figure 7).

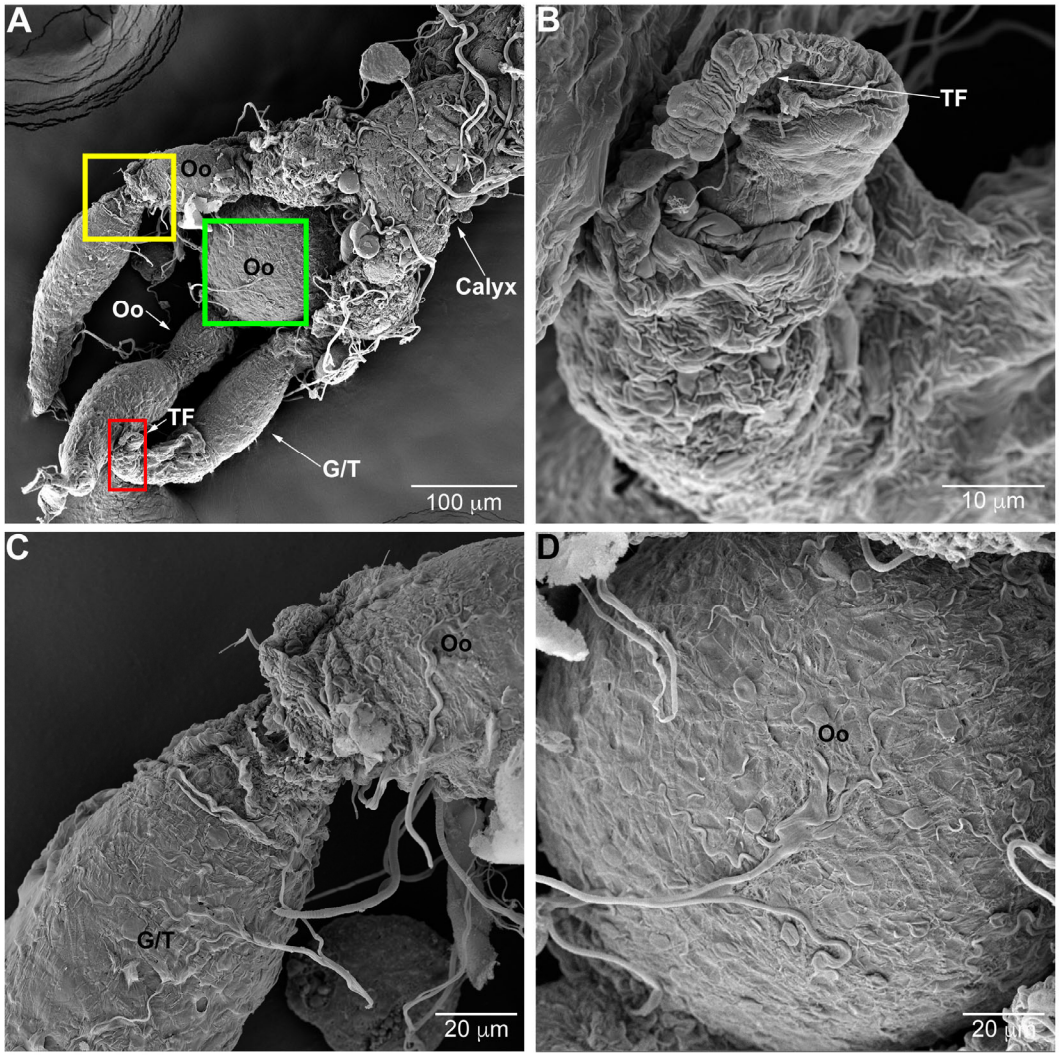

Figure 7. Structural organization of the ovary in a four-day-old *Zabrotes subfasciatus* adult. Dissected ovaries were post-fixed in 1% osmium tetroxide, washed, ethanol-dehydrated, CO_2 critical point–dried, and gold-coated (20 nm). Imaging was performed with a TESCAN-MIRA4 FEG SEM. A) Whole ovary showing the three ovarioles, oocytes, germarium/tropharium and the calyx. B) Terminal filament (red label in A). C) Germarium-vitellarium transition zone (yellow label in A). D) Oocyte within the vitellarium (green label in A). G/T, germarium/tropharium; Oo, oocyte; TF, terminal filament.

3.5. Histological Organization of the Larval Testis of Zabrotes subfasciatus

Light microscopy revealed that the testes of *Z. subfasciatus* larvae (14 days after oviposition) are in the posterior-middle region of the abdomen and are embedded within abundant fat body tissue (Figure 8). There are a pair of testes, each one formed by two follicles or lobes. The follicles are filled with numerous seminiferous cysts, each containing germ cells in the same stage of spermatogenesis (Figure 8C-F). The most anterior region contains germ cells and clusters of spermatogonia, indicating active mitotic proliferation. Spermatogonia appear as small, densely stained cells with prominent nuclei. Their anterior localization is characteristic of insect testes, where early germ-cell development occurs in defined germinal zones. More centrally, larger spermatocytes are observed. These cells

 doi:10.20944/preprints202607.2205.v1

exhibit increased cytoplasmic volume and larger well-stained or clear nuclei, consistent with progression toward meiosis. The presence of numerous spermatocytes demonstrates that germ-cell differentiation is well advanced during the larval stage. Several cysts contain spermatids, recognizable by their smaller size, condensed nuclei and a chromophobic, unstained circular area resembling a large vacuole, representing specialized cytoplasm area undergoing remodeling during spermiogenesis. While H&E morphology and cyst architecture strongly support the presence of post-meiotic cells in larvae, unequivocal discrimination of late spermatocytes from early spermatids requires ultrastructural or stage-specific marker validation. Their occurrence indicates meiosis in several cysts and is consistent with initiation of spermiogenesis before pupation; ultrastructural or marker validation is warranted. Overall, the larval testis exhibits the cystic organization characteristic of Coleoptera. Each germ-cell cyst is enclosed by elongated cyst cells, which surround groups of synchronously developing germ cells and provide structural and physiological support. Each testicular follicle also contains a centrally located lumen, consistent with an intrafollicular efferent duct that becomes enlarged distally (Figure 8C-F). However, because duct identity was inferred solely from its morphology and anatomical position in histological sections, and neither serial three-dimensional reconstruction nor duct-specific labeling was performed, alternative interpretations (e.g., tracheoles) cannot be completely excluded.

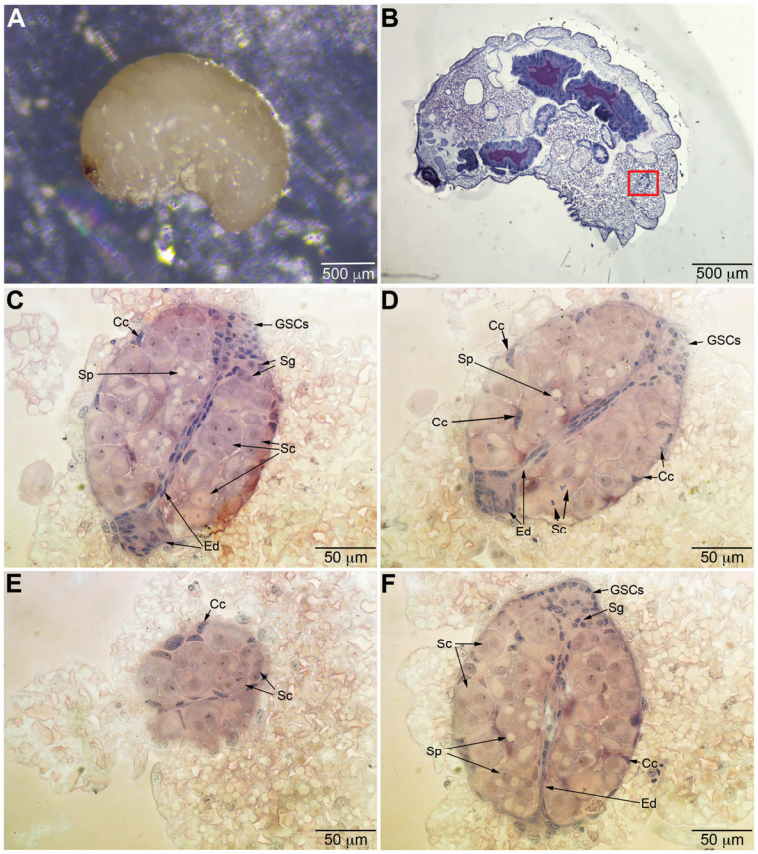

Figure 8. Histological organization of the larval (14 days after egg laying) testes of *Zabrotes subfasciatus*. A) Larva photographed using a ZEISS Stemi 305 stereomicroscope equipped with an Axiocam 105 colour camera and ZEN 3.7 software. Whole bodies (B) and dissected testes (C–F) were embedded in Historesin, sectioned at 5 µm, stained with haematoxylin and eosin, and imaged using a Nikon Eclipse 80i microscope equipped with a digital camera and NIS-Elements 3.1 software. B) Longitudinal section of a larval body highlighting the anatomical location of the testes (red label). GC, germ cell; Cc, cyst cell; Sp, differentiating spermatids; GSCs, germline stem cells; Sg, spermatogonia; Sc, spermatocytes; Ed, efferent duct.

 doi:10.20944/preprints202607.2205.v1

3.6. Histological Organization of the Late Larval (Pharate Pupae) Testes of Zabrotes subfasciatus

Compared with early larval testes, pharate-pupal testes appear enlarged in our histological sections and exhibit a qualitatively higher degree of differentiation (Figure 9). At this stage, numerous sperm bundles are readily observed within the testicular follicles (Figure 9E, F), consistent with advanced spermiogenesis. Concomitantly, the proportion of early germ-cell stages is markedly reduced, whereas post-meiotic cells, particularly spermatids and sperm bundles, predominate. The organization of the germ-cell cysts reflects progressive testicular maturation during metamorphosis, characterized by active spermiogenesis and the accumulation of differentiating spermatozoa. The predominance of late spermatogenic stages, together with the relative scarcity of proliferative germ cells, indicates that spermatogenesis is well advanced by the pharate-pupal stage. Although the pharate-pupal testes appear larger and contain more sperm bundles than those of larvae, these observations are qualitative, as neither testis volume nor sperm bundle density was quantified.

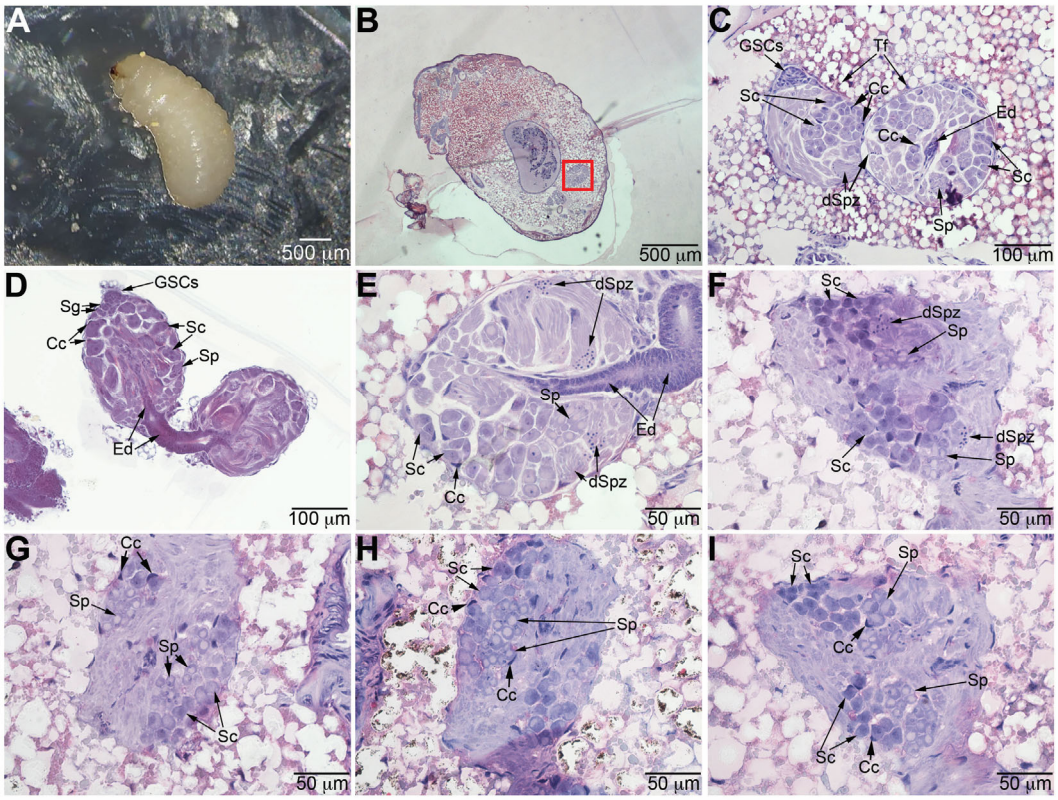

Figure 9. Histological organization of the pharate-pupal (20–22 days after egg laying) testes of *Zabrotes subfasciatus*. A) Pharate pupa photographed using a ZEISS Stemi 305 stereomicroscope equipped with an Axiocam 105 colour camera and ZEN 3.7 software. Whole bodies and dissected testes were embedded in Historesin, sectioned at 5 µm, stained with haematoxylin and eosin, and imaged using a Nikon Eclipse 80i microscope equipped with a digital camera and NIS-Elements 3.1 software (B–I). B) Longitudinal section of a pharate-pupal body highlighting the anatomical location of the testes (red label). C–I, magnified views of distinct sections from the red-labelled area indicated in B, though in C and D follicle (lobe) pairs are shown. GSCs, germline stem cells; Sc, spermatocytes; Cc, cyst cell; Tf, testicular follicle; Sp, differentiating spermatids; Ed, efferent duct (intrafollicular and extrafollicular portions are seen in D and E); Sg, spermatogonia; dSpz, differentiating spermatozoa.

3.7. Histological Organization of the Early Pupal Testes of Zabrotes subfasciatus

Early pupal testes contain, in addition to germ stem cells and cysts representing different stages of spermatogenesis and spermiogenesis, numerous dense bundles of spermatozoa (Figure 10C, D, F,

 doi:10.20944/preprints202607.2205.v1

H). These conspicuous structures are frequently observed in association with the intrafollicular efferent duct, suggesting the progressive establishment of sperm transport pathways within the reproductive tract. The abundance of spermatids and differentiating spermatozoa indicates intense spermiogenesis and ongoing sperm maturation. The simultaneous presence of meiotic cells (see dividing spermatocytes in E and F), post-meiotic spermatids, and sperm bundles demonstrates that the testis remains highly active, with multiple waves of spermatogenesis occurring concurrently. The predominance of spermatids and sperm bundles, coupled with the relative scarcity of early germ-cell stages, indicates that testicular maturation is nearing completion and that the reproductive system is being prepared for adult reproductive function.

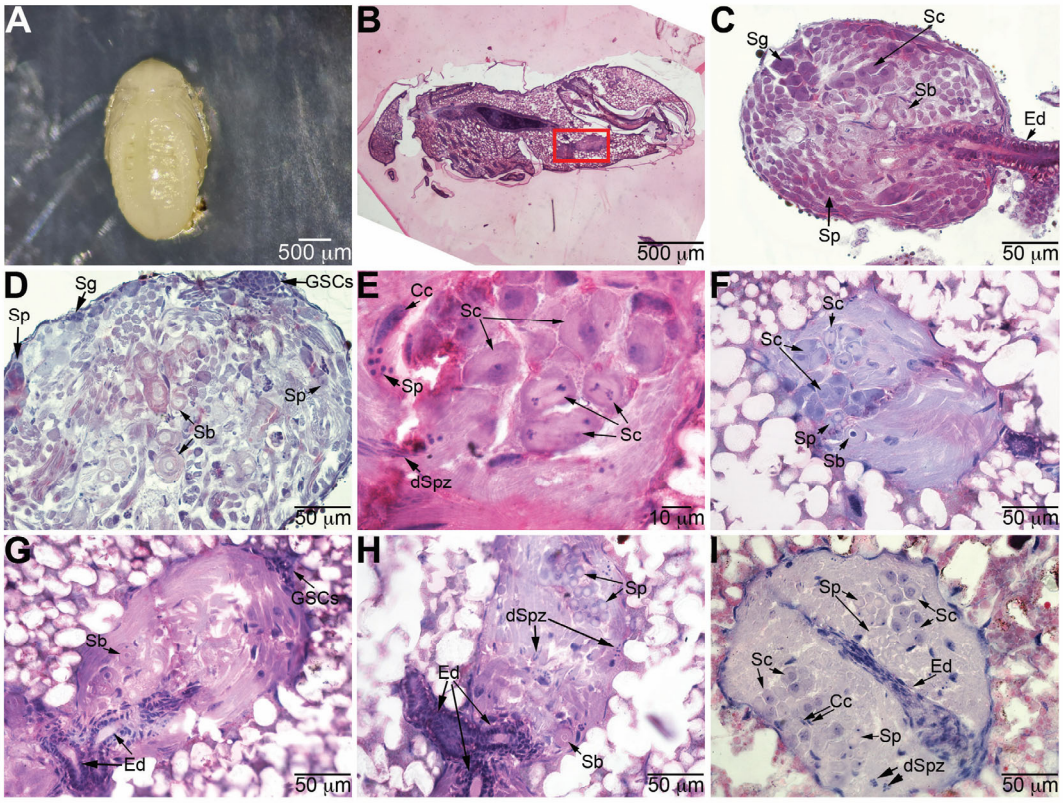

Figure 10. Histological organization of the pupal (20–22 days after egg laying) testes of *Zabrotes subfasciatus*. A) Pupa photographed using a ZEISS Stemi 305 stereomicroscope equipped with an Axiocam 105 colour camera and ZEN 3.7 software. Whole bodies and dissected testes (C–D) were embedded in Historesin, sectioned at 5 µm, stained with haematoxylin and eosin, and imaged using a Nikon Eclipse 80i microscope equipped with a digital camera and NIS-Elements 3.1 software. B) Longitudinal section of a pupal body highlighting the anatomical location of the testes (red label). C–I, magnified views of distinct sections from the red-labelled area indicated in B. Cc, cyst cell; Sp, spermatids; GSCs, germline stem cells; Sg, spermatogonia; Sc, spermatocytes; Ed, efferent duct (intrafollicular and extrafollicular portions); Tf, testicular follicle; dSpz, differentiating spermatozoa; Sb, sperm bundles.

3.8. Histological Organization of the Pharate-Adult Testes of Zabrotes subfasciatus

Pharate-adult testes show coexisting spermatogenic stages (Figure 11), consistent with asynchronous development, although organ-wide quantification was not performed. In addition, small groups of cyst cells remain associated with same-stage groups of germ cells. The presence of multiple developmental stages within adjacent cysts indicates continuous and already highly active spermatogenesis (Figure 11).

 doi:10.20944/preprints202607.2205.v1

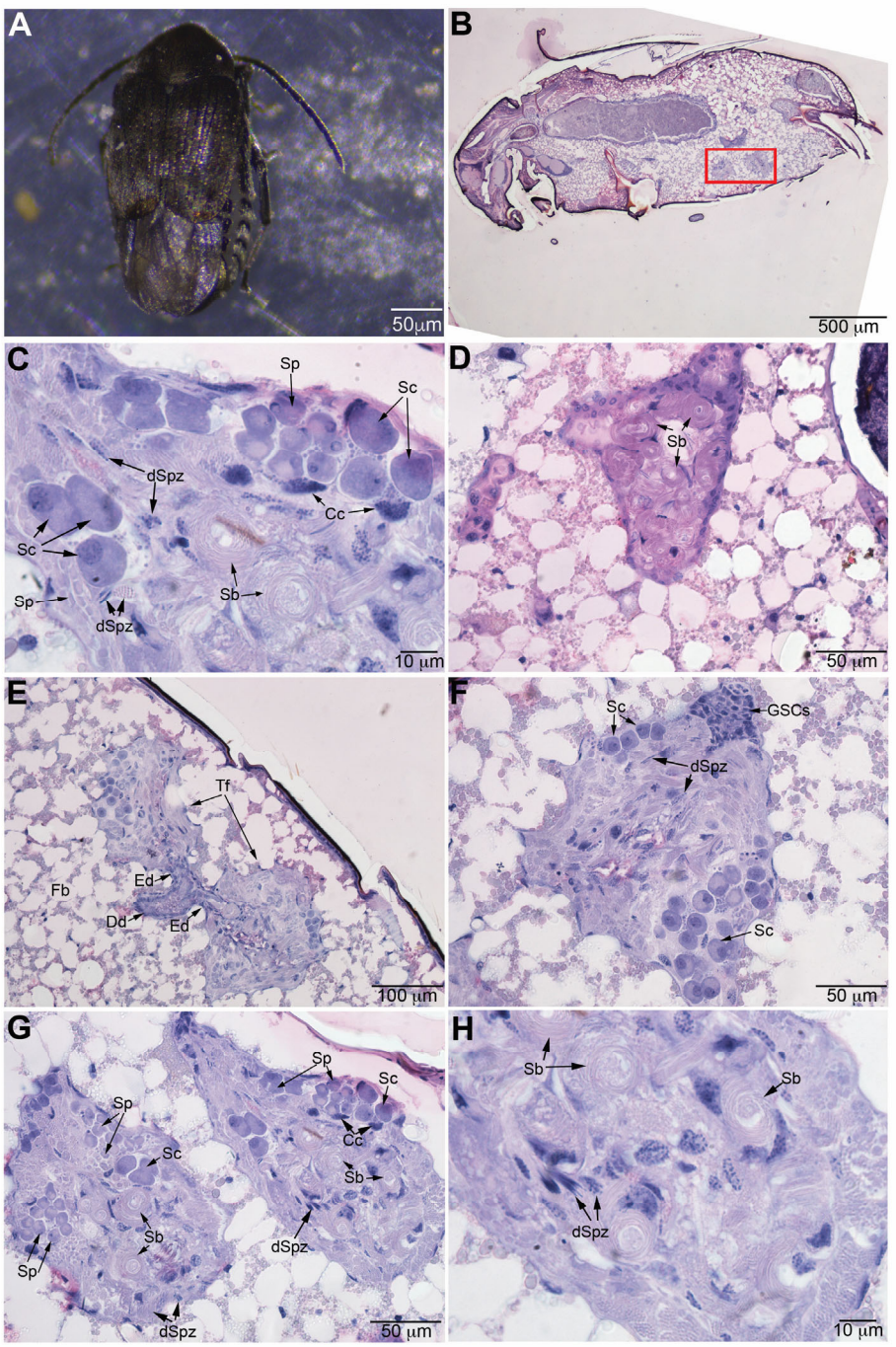

Figure 11. Histological organization of the pharate-adult (24–25 days after egg laying) testes of *Zabrotes subfasciatus*. A) Pharate adult photographed using a ZEISS Stemi 305 stereomicroscope equipped with an Axiocam 105 colour camera and ZEN 3.7 software. Whole bodies were embedded in Historesin, sectioned at 5 µm, stained with haematoxylin and eosin, and imaged using a Nikon Eclipse 80i microscope equipped with a digital camera and NIS-Elements 3.1 software. B) Longitudinal section of a pharate-adult body highlighting the anatomical location of the testes (red label). C–H, magnified views of distinct sections from the red-labelled area indicated in B. Cc, cyst cell; Sp, spermatids; GSCs, germline stem cells; Sc, spermatocytes; Ed, efferent duct; Dd, deferent duct; Tf, testicular follicle; dSpz, differentiating spermatozoa; Sb, sperm bundles; Fb, fat body.

 doi:10.20944/preprints202607.2205.v1

3.9. Histological Organization of the Adult Testis of Zabrotes subfasciatus

Histological sections of four-day-old testes reveal fully differentiated gonads with coexisting spermatogenic stages and many sperm bundles; functional activity and sperm viability were not assayed. Different developmental stages of the germ line coexist within the testicular follicles, indicating continuous sperm production in the sexually mature male (Figure 12).

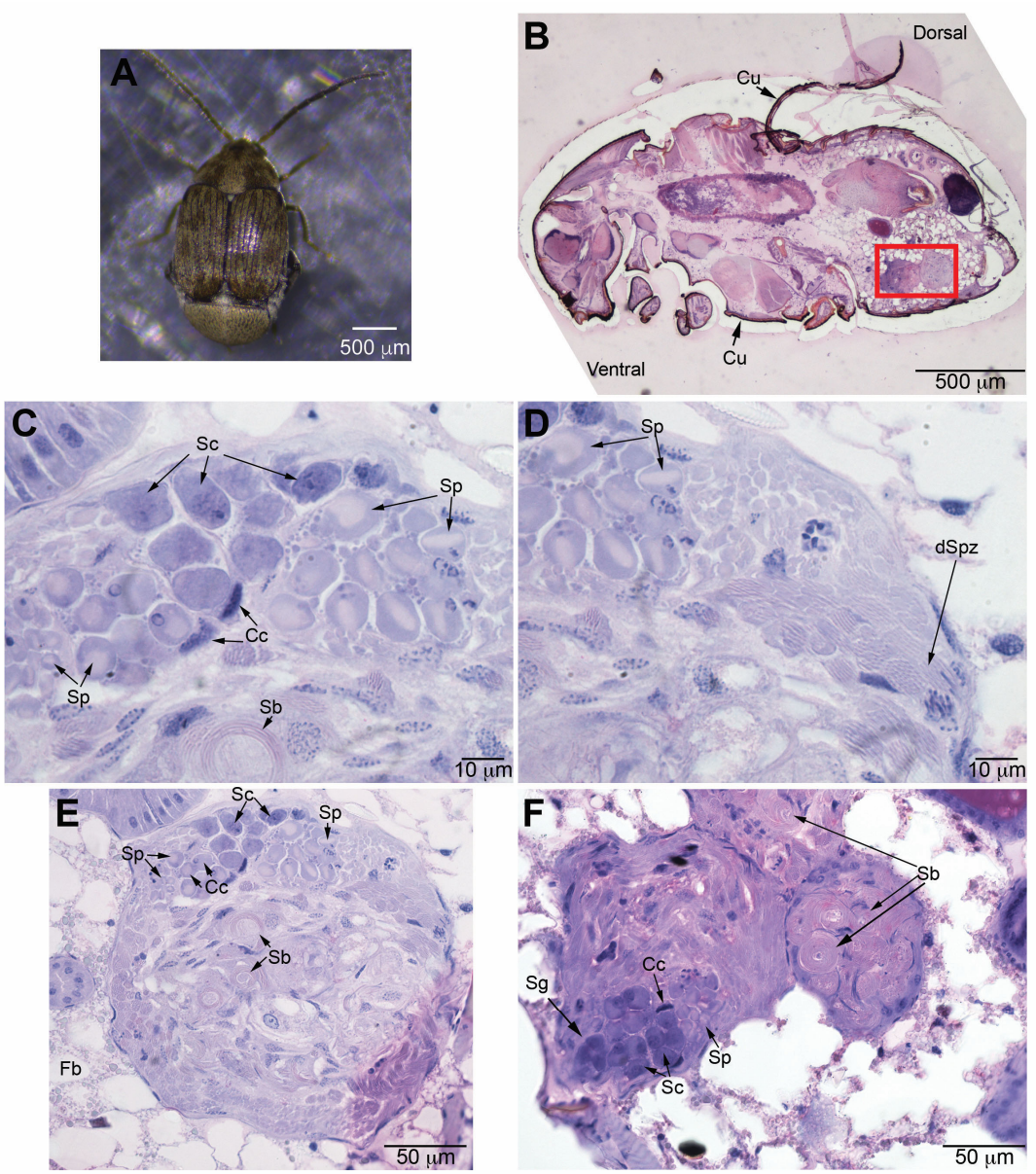

Figure 12. Histological organization of the testes in a four-day-old *Zabrotes subfasciatus* adult. A) Adult photographed using a ZEISS Stemi 305 stereomicroscope equipped with an Axiocam 105 colour camera and ZEN 3.7 software. Whole bodies were embedded in Historesin, sectioned at 5 μm, stained with haematoxylin and eosin, and imaged using a Nikon Eclipse 80i microscope equipped with a digital camera and NIS-Elements 3.1 software. B) Longitudinal section of an adult body highlighting the anatomical location of the testes (red label). C–F, magnified views of distinct sections from the red-labelled area indicated in B. Cu, cuticle; Sc, spermatocytes; Sp, differentiating spermatids; Cc, cyst cell; Sb, sperm bundles; Sg, spermatogonia; dSpz, differentiating spermatozoa; Fb, fat body.

 doi:10.20944/preprints202607.2205.v1

The male reproductive system of a four-day-old adult *Z. subfasciatus*, observed under stereomicroscopy, exhibits a fully differentiated reproductive apparatus indicative of active sperm production, storage, and reproductive readiness. The paired testes are each composed of rounded follicles (lobes) that connect medially to the seminal vesicles, which likely function in the storage of sperm released from the follicles. Posteriorly, the reproductive tract continues through the deferent ducts and ejaculatory duct, while a pair of well-developed accessory glands is associated with its distal region (Figure 13A, B). Light microscopy confirms the bilobed organization of each testis and reveals densely packed cellular contents corresponding to germ cells at different stages of spermatogenesis, as well as the presence of sperm bundles, indicating intense spermatogenic activity and sperm accumulation (Figure 13B). Scanning electron microscopy further illustrates the three-dimensional organization of the reproductive system, highlighting the compact arrangement of the follicles, accessory glands, and ejaculatory duct, as well as the smooth to slightly folded surface of the follicular sheath (Figure 13C). Together with the histological evidence presented in the previous figures, these observations demonstrate that male reproductive maturation is completed within four days after adult emergence, when the reproductive system appears fully functional. However, since we did not directly assay adult germ-cell proliferation, apoptosis, sperm motility, or sperm viability; therefore, "active" spermatogenesis and functional competence are inferred from morphology.

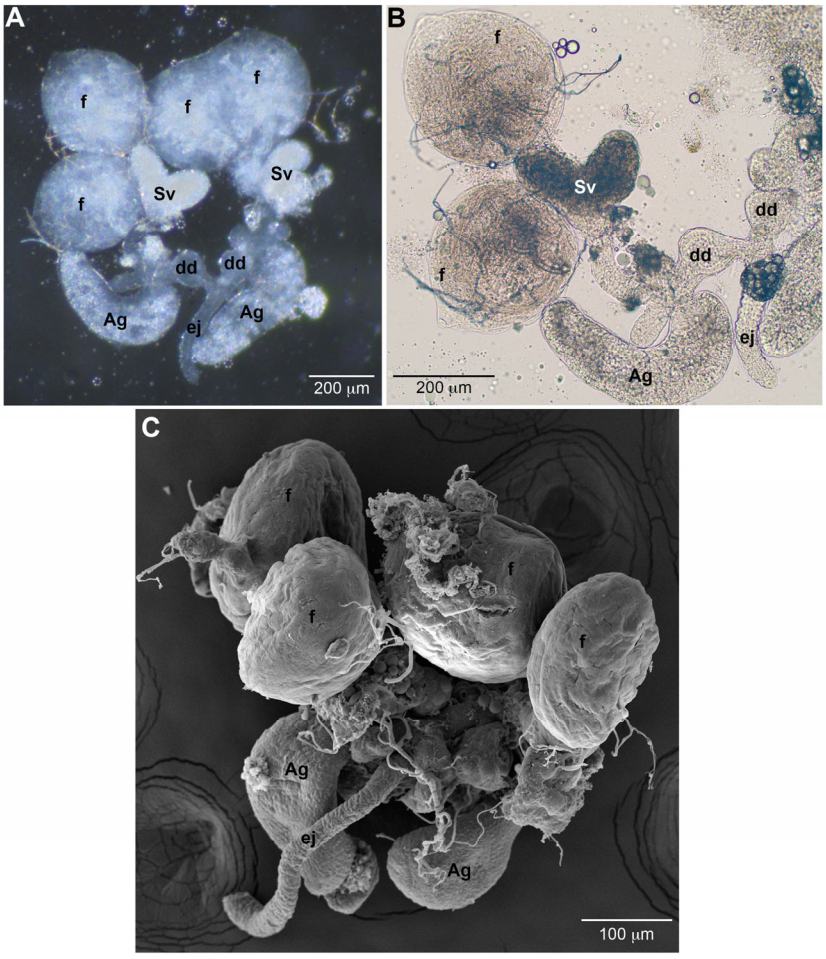

Figure 13. Structural organization of the reproductive system of a four-day-old *Zabrotes subfasciatus* adult male. A) Dissected testes and reproductive structures were mounted on microscope slides containing PBS and photographed using a STEMI 305 stereomicroscope (Zeiss). B) The slide with dissected reproductive system was placed under an Olympus CX21 microscope and photographed using an AmScope MU1003 camera. C) Tissues were post-fixed in 1% osmium tetroxide, washed, ethanol-dehydrated, CO_2 critical point-dried, and gold-coated

 doi:10.20944/preprints202607.2205.v1

(20 nm). Imaging was performed with a TESCAN-MIRA4 FEG SEM. F, testicular follicle; Sv, seminal vesicle; dd, deferent duct; Ag, accessory gland; ej, ejaculatory duct.

4. Discussion

Using stereomicroscopy, light microscopy, and scanning electron microscopy, we establish a stage-by-stage morphological framework for gonad maturation in *Z. subfasciatus*. Our analyses reveal that post-embryonic gonad development begins during larval life but reaches its principal structural and functional organization during late metamorphosis. This developmental trajectory supports the hypothesis that reproductive readiness in this capital-breeding seed beetle is established before adult emergence, rather than being deferred until adulthood. In females, the larval and pharate-pupal ovaries are characterized primarily by proliferative germaria and posterior duct-like regions, whereas the defining features of telotrophic meroistic ovarioles become evident during the pupal-to-pharate-adult transition. The differentiation of individualized oocytes, follicular cells, trophic cords, a distinct vitellarium, and the onset of yolk deposition before adult emergence indicates that ovarian maturation is already underway during the pharate-adult stage. This interpretation is further supported by the establishment of a clear germarium-vitellarium transition, follicular encapsulation of developing oocytes, and fully regionalized adult ovarioles. Although we did not employ molecular or ultrastructural approaches to confirm yolk identity or the ultrastructure of trophic cords, the observed morphological changes strongly indicate the onset of ovarian function before adult emergence. These findings are consistent with previous evidence showing that vitellogenesis in *Z. subfasciatus* begins during late metamorphosis and that subsequent ovarian activation is modulated by host seeds and male presence after adult emergence (Miranda et al., 2025).

The ovarian sequence described here clarifies how the adult telotrophic architecture is assembled during metamorphosis. In telotrophic meroistic ovarioles, nurse-cell and germ stem cell derivatives remain concentrated in the tropharium, while developing oocytes remain connected to this region by trophic cords and are progressively enclosed by follicular cells (Leyria, 2024). In *Z. subfasciatus*, this organization is only weakly defined in larvae and pupae, but becomes evident in pharate adults, when the transition between tropharium and vitellarium can be recognized. Thus, the pupal-to-pharate-adult interval appears to be the critical morphogenetic window for establishing the functional compartments of the ovary. The convergence of the posterior duct-like regions of the three ovarioles into a common terminal structure during pharate-pupal and pupal development likely represents formation of the future calyx. Comparable differentiation of ovariole pedicels and associated duct systems has been described in insects with telotrophic ovaries, including *Triatoma infestans* and *Rhodnius prolixus* (Mariano et al., 2004, 2008; Lange et al., 2022), as well as in the curculionid *Hyperodes bonariensis* (Goldson and Emberson, 1981). In *Z. subfasciatus*, completing this ductal integration before emergence may facilitate the rapid transition from ovarian maturation to effective oviposition.

Male gonad development follows a similarly early, but more continuously progressive, trajectory. The larval testis is not an undifferentiated gonad; it already contains germ stem cells, spermatogonia, spermatocytes, spermatids, cyst cells, and intrafollicular efferent ducts. The presence of spermatids indicates that meiotic divisions have occurred and that spermiogenesis begins before pupation. Spermatids are characterized by a condensed nucleus and a chromophobic cytoplasm area, which typically corresponds to the nebenkern, an spherical structure, histologically similar to a large vacuole, but derived from aggregation and fusion of the entire spermatid mitochondrial complement. Its chemical composition reflects that of mitochondrial membranes, enriched with lipids. This makes the nebenkern poorly stained with the histological dyes we used here, hematoxylin and eosin (Bowen, 1922; Vedelek et al., 2024). This early gonad organization suggests that the basic architecture of the male reproductive tract is established during larval life, although full functional integration is completed later. The close association between testes and fat body tissue further supports the high energetic demands of germ-cell proliferation and differentiation. Overall, the larval testis exhibits the

 doi:10.20944/preprints202607.2205.v1

cystic organization characteristic of Coleoptera (e.g., Mukerji and Bhuya, 1937) and demonstrates that male gametogenesis is already advanced before metamorphosis.

During the pharate-pupal and pupal stages, testicular maturation becomes even more pronounced. The abundance of spermatids, differentiating spermatozoa, and dense sperm bundles indicates that spermiogenesis is the predominant process during this interval. In early pupae, the accumulation of elongating sperm bundles near the intrafollicular efferent duct suggests that sperm transport pathways are being established and that the reproductive tract is approaching functional integration. This pattern resembles the precocious development reported for other insects, in which substantial sperm production occurs before adult emergence (e.g., Lago et al., 2020). For *Z. subfasciatus*, early spermatogenic progression is likely adaptive because adults are short-lived and initiate reproductive activity soon after emergence (Teixeira et al., 2008; Teixeira et al., 2016; Miranda et al., 2025). By the pharate-adult stage, testes contain multiple spermatogenic stages simultaneously, consistent with asynchrony; however, lobe-wide staging was not quantified. Four-day-old adult males show a fully differentiated reproductive system, including compact testicular follicles, seminal vesicles, deferent ducts, accessory glands, and the ejaculatory duct. The persistence of early germ cells together with abundant sperm bundles indicates that sperm production continues after emergence, ensuring a continuous sperm supply during adult reproductive life.

Together, the female and male data indicate that metamorphosis in *Z. subfasciatus* does more than enlarge pre-existing gonadal structures: it reorganizes proliferative larval organs into compartmentalized reproductive systems that are largely prepared for function by adult emergence (Miranda et al., 2025). This developmental schedule fits the biology of Bruchinae, whose larvae develop within seeds and whose adults frequently rely on larval reserves to support reproduction (Southgate, 1979). Under this life-history strategy, early gonad maturation may reduce the delay between emergence, mating, and oviposition, thereby increasing reproductive efficiency in a pest species with a short adult lifespan (Teixeira et al., 2008).

5. Conclusion

This study demonstrates that gonad development in *Z. subfasciatus* is initiated during larval life and becomes functionally organized mainly during late metamorphosis. In females, the transformation from proliferative larval ovarioles to an adult-like telotrophic meroistic organization occurs chiefly between the pupal and pharate-adult stages, when germarial and vitellogenic regions become distinguishable, follicular cells and trophic cords appear, and vitellogenesis begins before adult emergence. In males, testicular differentiation is also advanced before emergence, with larval testes already containing multiple germ-cell stages and later stages showing intense spermiogenesis, sperm-bundle accumulation, and differentiation of the reproductive tract (Figure 14). Together, these findings support the hypothesis that reproductive readiness in this capital-breeding seed beetle is developmentally anticipated rather than delayed until adult life. By integrating female and male gonad ontogeny across post-embryonic development, this work provides a morphological framework for understanding the rapid onset of reproduction in newly emerged adults and establishes a basis for future studies on endocrine regulation, reproductive ecology, and strategies aimed at disrupting reproduction in this economically important pest.

 doi:10.20944/preprints202607.2205.v1

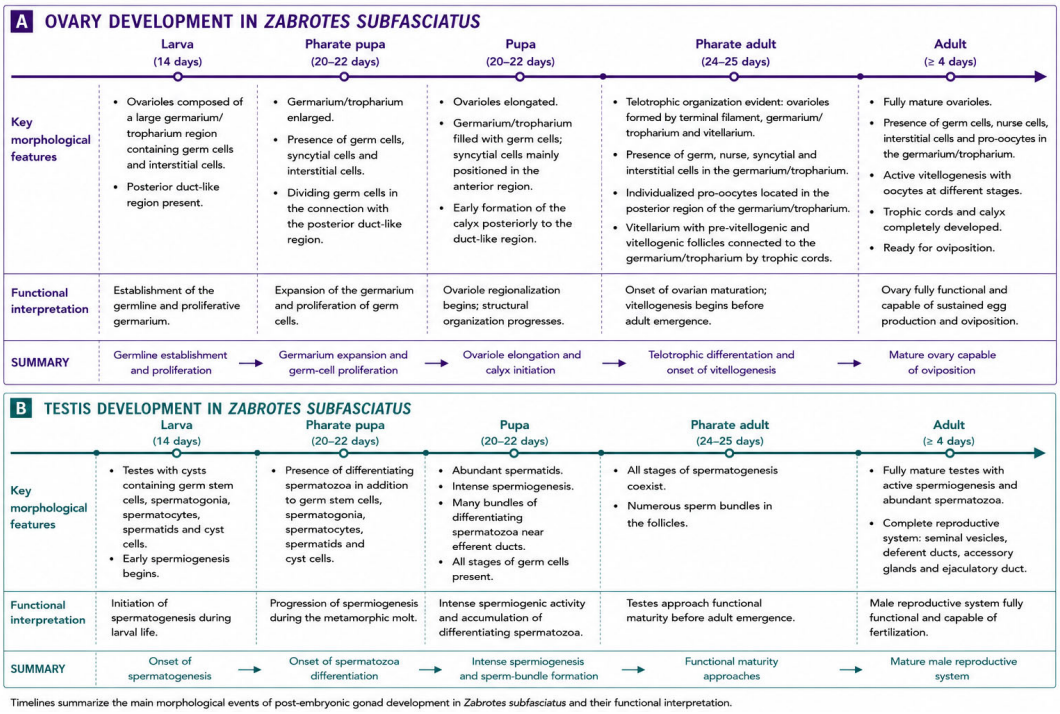

Figure 14. Timeline of post-embryonic gonad development in *Zabrotes subfasciatus*. The upper timeline summarizes the major morphological events during ovary development, whereas the lower timeline shows the corresponding stages of testis development. Developmental stages are arranged chronologically according to age after egg laying: larva (14 days), pharate pupa (20-22 days), pupa (20-22 days in females; early and late pupal stages in males), pharate adult (24-25 days), and adult (4 days after emergence). In females, A, ovarian development progresses from proliferative germaria and undifferentiated ovarioles to the establishment of a telotrophic meroistic organization, with oocyte differentiation, formation of follicular cells and trophic cords, and the onset of vitellogenesis before adult emergence. In males, B, testicular development is characterized by progressive spermatogenesis, increasing abundance of spermatids and sperm bundles, differentiation of the reproductive tract, and completion of reproductive maturation shortly after adult emergence. Days indicate the approximate age after egg laying under the rearing conditions used in this study.

Author Contributions: Conceptualization, J.R.M., M.M.G.B. and A.R.B.; Methodology, J.R.M. and M.M.G.B.; Investigation, J.R.M. and S.O.M.; Resources, T.S.M. and A.R.B.; Data Curation, J.R.M. and M.M.G.B.; Writing-Original Draft Preparation, A.R.B.; Writing-Review and Editing, J.R.M., M.M.G.B., T.S.M., S.O.M., and A.R.B.; Visualization, J.R.M.; Supervision, T.S.M. and A.R.B.; Project Administration, A.R.B.; Funding Acquisition, A.R.B. All authors have read and agreed to the published version of the manuscript.

Funding: Financial support was provided by the Fundação de Amparo à Pesquisa do Estado de Minas Gerais (FAPEMIG Grant Proc. # APQ-00325-22), Conselho Nacional de Desenvolvimento Científico e Tecnológico (CNPq Grant Proc. # 404696/2021-0; CNPq Fellowships Proc. # 307847/2021-7; 304957/2024-0), and the Coordenação de Aperfeiçoamento de Pessoal de Nível Superior-Brasil (CAPES)-Finance Code 001. We are also grateful to institutional grants provided by FINEP-Financiadora de Estudos e Projetos. The funders had no role in study design, data collection and analysis, decision to publish, or preparation of the manuscript.

Data Availability Statement: The original contributions presented in this study are included in the article. Further inquiries can be directed to the corresponding author.

Acknowledgments: We thank Thalles Henrique Faria de Souza (CEMIC/UNIFAL-MG) for performing the scanning electron microscopy (SEM) processing and imaging, and Isabel R. V. Teixeira for her assistance with Figure 14.

 doi:10.20944/preprints202607.2205.v1

Conflicts of Interest: The authors declare that they have no known competing financial interests or personal relationships that could have appeared to influence the work reported in this paper.

Declaration on the Use of Artificial Intelligence Tools: During the preparation of this manuscript, the authors used Microsoft Copilot (for Microsoft 365) to assist with grammar correction and reference formatting, and ChatGPT (OpenAI, GPT-5.5) to assist in the design and wording of the developmental timeline presented in Figure 14. Following the use of these tools, the authors critically reviewed, edited, and verified all generated content and take full responsibility for the accuracy and integrity of the final manuscript.

References

Boheman, C.H. Genera et species Curculionidum, cum synonymia hujus familiae. In *Synonymia Insectorum, Oder: Versuch Einer Synonymie Aller Bisher Bekannten Insecten; Nach Fabricii Systema Eleutheratorum & c. Geordnet*; Schoenherr, C.J., Ed.; Roret: Paris, France, **1833**.

Bondar, G.G. Notas biologicas sobre bruchideos observados no Brasil. *Jornal do Commercio*: Rio de Janeiro, Brazil, **1937**.

Bowen R. H. Studies on insect spermatogenesis. iii. On the structure of the nebenkern in the insect spermatid and the origin of nebenkern patterns. Biological Bulletin **1922**, 42 (2), 53-84.

Corrêa, C.P.; Capizzani, B.C.; Beijo, L.A.; Ávila, P.M.; Teixeira, I.R.V.; Barchuk, A.R. Adult feeding and host type modulate the life history traits of the capital breeder *Zabrotes subfasciatus*. *Physiological Entomology* **2020**, *45*, 120–128.

Corrêa, C.P.; Parreiras, S.S.; Beijo, L.A.; Ávila, P.M.; Teixeira, I.R.V.; Barchuk, A.R. Life history trait response to ambient temperature and food availability variations in the bean weevil *Zabrotes subfasciatus*. *Physiological Entomology* **2021**, *46*, 189–199.

Cruz, B.O.; Miranda, S.O.; Benedito, E.R.C.; Martins, J.R.; Caixeta, E.S.; Beijo, L.A.; Mazzoni, T.S.; Moda, L.M.R.; Teixeira, I.R.V.; Barchuk, A.R. Early adaptation to an unusual host in the bean weevil *Zabrotes subfasciatus* is associated with changes in body size and reproductive physiology. *Physiological Entomology* **2026**, *51*, 147–162. doi:10.1111/phen.70011.

Gerber, G. H. A possible mechanism for the regulation of the female reproductive cycle in *Tenebrio molitor* (Coleoptera: Tenebrionidae). The Canadian Entomologist, **1967**, 99(12), 1298–1303. https://doi.org/10.4039/Ent991298-12

Goldson, S.L.; Emberson, R.M. Reproductive morphology of the Argentine stem weevil, *Hyperodes bonariensis* (Coleoptera: Curculionidae). *New Zealand Journal of Zoology* **1981**, *8*, 67–77. doi:10.1080/03014223.1981.10427942.

Harris, H.F. On the rapid conversion of haematoxylin into haematein in staining reactions. *Journal of Applied Microscopy and Laboratory Methods* **1900**, *3*, 777.

Howe, R.W.; Currie, J.E. Some laboratory observations on the rates of development, mortality and oviposition of several species of Bruchidae breeding in stored pulses. *Bulletin of Entomological Research* **1964**, *55*, 437–477.

Jönsson, K.I. Capital and income breeding as alternative tactics of resource use in reproduction. *Oikos* **1997**, *78*, 57. doi:10.2307/3545800.

Karnovsky, M.J. A formaldehyde-glutaraldehyde fixative of high osmolality for use in electron microscopy. *Journal of Cell Biology* **1965**, *27*, 1A–149A.

Kiernan, J.A. Histological and histochemical methods: theory and practice. 5th ed. Newbury: Scion Publishing; 2015.

Kingsolver, J.M. *Handbook of the Bruchidae of the United States and Canada (Insecta: Coleoptera)*; USDA Technical Bulletin 1912; United States Department of Agriculture: Washington, DC, USA, **2004**; Volume 1, pp. 1–324.

Kutcherov, D. Stagewise resolution of temperature-dependent embryonic and postembryonic development in the cowpea seed beetle *Callosobruchus maculatus* (F.). *BMC Ecology* **2020**, *20*, 50. doi:10.1186/s12898-020-00318-2.

Lago, D.C.; Martins, J.R.; Dallacqua, R.P.; *et al.* Testis development and spermatogenesis in drones of the honey bee, *Apis mellifera* L. *Apidologie* **2020**, *51*, 935–955. doi:10.1007/s13592-020-00773-2.

Lange, A.B.; Leyria, J.; Orchard, I. The hormonal and neural control of egg production in the historically important model insect, *Rhodnius prolixus*: A review, with new insights in this post-genomic era. *General and Comparative Endocrinology* **2022**, *321–322*, 114030. doi:10.1016/j.ygcen.2022.114030.

Leyria, J. Endocrine factors modulating vitellogenesis and oogenesis in insects: An update. *Molecular and Cellular Endocrinology* **2024**, *587*, 112211. doi:10.1016/j.mce.2024.112211.

Lucas, M.H. *Spermophagus semifasicatus*. *Annales de la Société Entomologique de France* **1858**, série 3, tome 6, 245–248.

 doi:10.20944/preprints202607.2205.v1

Lussier, J.; Racine, E.; Benoit-Biancamano, M.-O. Histology of the whole body of honey bees: Tissue fixation and processing. *Journal of Veterinary Diagnostic Investigation* **2023**, *35*, 625–629. doi:10.1177/10406387231160767.

Mariano, M.I.; Ibáñez, C.I.; Bozzini, J.P. Differentiation and morphogenesis of *Triatoma infestans* (Klug 1834) female gonads. I—post embryonic development. *Biocell* **2004**, *28*, 259–269.

Mariano, M.I.; Ibáñez, C.I.; Bozzini, J.P. Post-embryonic development of ovariole pedicels in *Triatoma infestans* (Klug 1834): A morphometrical approach. *Acta Microscopica* **2008**, *17*, 28–38.

Miranda, S.O.; Cruz, B.O.; Martins, J.R.; Mazzoni, T.S.; Miranda, W.O.; Moda, L.M.R.; Caixeta, E.S.; Teixeira, I.R.V.; Barchuk, A.R. Ovary activation dynamics in the bean weevil *Zabrotes subfasciatus* (Bruchinae): The essential roles of seeds and males. *Insects* **2025**, *16*, 894. doi:10.3390/insects16090894.

Mukerji, D.; Bhuya, M.A.H. Reproductive system of the bruchid beetles *Bruchus quadrimaculatus* Fabr., *Bruchus* (*Callosobruchus*) *chinensis* L. (Bruchidae—Coleoptera). *Journal of Morphology* **1937**, *61*, 175–214.

Schoch, C.L.; Ciufo, S.; Domrachev, M.; Hotton, C.L.; Kannan, S.; Khovanskaya, R.; Leipe, D.; McVeigh, R.; O'Neill, K.; Robbertse, B.; *et al.* NCBI Taxonomy: A comprehensive update on curation, resources and tools. *Database* **2020**. doi:10.1093/database/baaa062.

Southgate, B.J. Biology of the Bruchidae. *Annual Review of Entomology* **1979**, *24*, 449–473.

Souza, G.A.; Carvalho, M.R.O.; Martins, E.R.; Guedes, R.N.C.; Oliveira, L.O. Diversidade genética estimada com marcadores ISSR em populações brasileiras de *Zabrotes subfasciatus*. *Pesquisa Agropecuária Brasileira* **2008**, *43*, 843–849.

Teixeira, I.R.V.; Barchuk, A.R.; Zucoloto, F.S. Host preference of the bean weevil *Zabrotes subfasciatus*. *Insect Science* **2008**, *15*, 335–341. doi:10.1111/j.1744-7917.2008.00218.x.

Teixeira, I.R.V.; Barchuk, A.R.; Medeiros, L.; Zucoloto, F.S. Females of the weevil *Zabrotes subfasciatus* manipulate the size and number of eggs according to the host seed availability. *Physiological Entomology* **2009**, *34*, 246–250. doi:10.1111/j.1365-3032.2009.00682.x.

Teixeira, I.R.V.; Beijo, L.A.; Barchuk, A.R. Behavioral and physiological responses of the bean weevil *Zabrotes subfasciatus* to intraspecific competition. *Journal of Stored Products Research* **2016**, *69*, 51–57.

Teixeira, I.R.V.; Gris, C.F. Genetic diversity of grains, storage pests and their effects on the worldwide bean supply. In *Beans: Nutrition, Consumption and Health*;

Popescu, E.; Golubev, I., Eds.; Nova Science Publishers: New York, NY, USA, **2011**.

Teixeira, I.R.V.; Zucoloto, F.S. Intraspecific competition in *Zabrotes subfasciatus*: Physiological and behavioral adaptations to different amounts of host. *Insect Science* **2012**, *19*, 102–111. doi:10.1111/j.1744-7917.2011.01425.x.

Tuda, M. Evolutionary diversification of bruchine beetles: Climate-dependent traits and development associated with pest status. *Bulletin of Entomological Research* **2011**, *101*, 415–422. doi:10.1017/S0007485310000660.

Valencia, C.A.; Cardona Mejía, C.; van Schoonhoven, A. *Main Insect Pests of Stored Beans and Their Control*; Centro Internacional de Agricultura Tropical (CIAT): Cali, Colombia, **1986**.

Vedelek, V.; Jankovics F.; Zádori J.; Sinka, R. Mitochondrial differentiation during spermatogenesis: lessons from Drosophila melanogaster. *International Journal of Molecular Sciences* **2024**, 25, 3980.

Wilson, D. S., & Knollenberg, W. G. Food discrimination and ovarian development in burying beetles (Coleoptera: Silphidae: Nicrophorus). Annals of the Entomological Society of America **1984**, 77(2), 165–170. https://doi.org/10.1093/aesa/77.2.165

Wu, L.-H.; Wang, C.-P.; Wu, W.-J. Description and differentiation of the four larval instars of *Acanthoscelides macrophthalmus* (Coleoptera: Chrysomelidae: Bruchinae). *Annals of the Entomological Society of America* **2012**, *105*, 259–267. doi:10.1603/AN11129.